

# Explanation of the RHIC $p_\perp$ -spectra in a thermal model with expansion

Wojciech Broniowski and Wojciech Florkowski  
*H. Niewodniczański Institute of Nuclear Physics, PL-31342 Cracow, Poland*

The freeze-out of the hadron gas on the hyper-surface  $\tau = \sqrt{t^2 - r_z^2 - r_x^2 - r_y^2}$  of limited transverse size,  $\sqrt{r_x^2 + r_y^2} < \rho_{\max}$ , explains the recently-measured RHIC  $p_\perp$ -spectra to a surprising accuracy. The original thermal spectra are supplied with secondary decays of resonances, and subsequently folded with the expansion. The predictions of this simple model are in qualitative and quantitative agreement with the available data.

25.75.-q, 25.75.Dw, 25.75.Ld

In this paper we offer a very simple explanation of the  $p_\perp$ -spectra recently measured at RHIC [1–3]. Our approach is a combination of the thermal model and Bjorken-like expansion supplied with transverse flow. In our model we do not need to distinguish the *chemical* and *thermal* freeze-outs – they occur simultaneously. So far, the thermal approach has been successfully applied in studies of particle ratios measured in relativistic heavy-ion collisions at AGS and SPS [4–9]. Quite recently, it has been shown that the particle ratios measured at RHIC may also be described in the framework of such models [10,11]. Description of the hadron  $p_\perp$ -spectra in thermal models is more involved, since the spectra are affected by the decays of resonances, hydrodynamic flow, and possibly by other phenomena occurring during the alleged phase transition from the quark-gluon plasma to a hadron gas [12]. The results of our simple model are in surprising agreement with experiment, *cf.* Fig. 1. The model has, except for the scale parameter  $\tau$ , essentially only one free parameter, the transverse radius at freeze-out, which is of the order of a few fm.

Here is the brief outline of our method. Following for instance Refs. [13–15], we assume that the freeze-out takes place at a fixed value of the invariant time,

$$\tau = \sqrt{t^2 - r_z^2 - r_x^2 - r_y^2} = \text{const}, \quad (1)$$

which means that the particles in the fluid elements moving farther away from the collision center decouple later than the particles in the fluid elements remaining at rest (in the center-of-mass system of the colliding nuclei). The local freeze-out conditions, *i.e.*, the values of the temperature and the chemical potentials, are universal for the whole freeze-out hyper-surface. Since the particle ratios at mid-rapidity are not affected by the expansion following from Eq. (1) (this important point is discussed below), the values of the thermodynamic parameters may be obtained from the standard thermal analysis which yields  $T = 165$  MeV,  $\mu_B = 41$  MeV,  $\mu_S = 9$  MeV, and  $\mu_I = -1$  MeV [11]. Knowing  $T$  and  $\mu$ 's we calculate the local distribution functions of hadrons which include the initial thermal contribution, as well as additional contributions from the sequential decays of *all* heavier reso-

nances. These decays are very important, since they effectively cool the system by 35–40 MeV, as recently shown in Ref. [11], and also known from earlier works on other reactions [16,17]. We limit the transverse size of the system with the condition  $\rho = \sqrt{r_x^2 + r_y^2} < \rho_{\max}$ . Finally, the standard Cooper-Frye-Schonberg formula [18] is used to calculate the  $p_\perp$ -spectra of the observed hadrons.

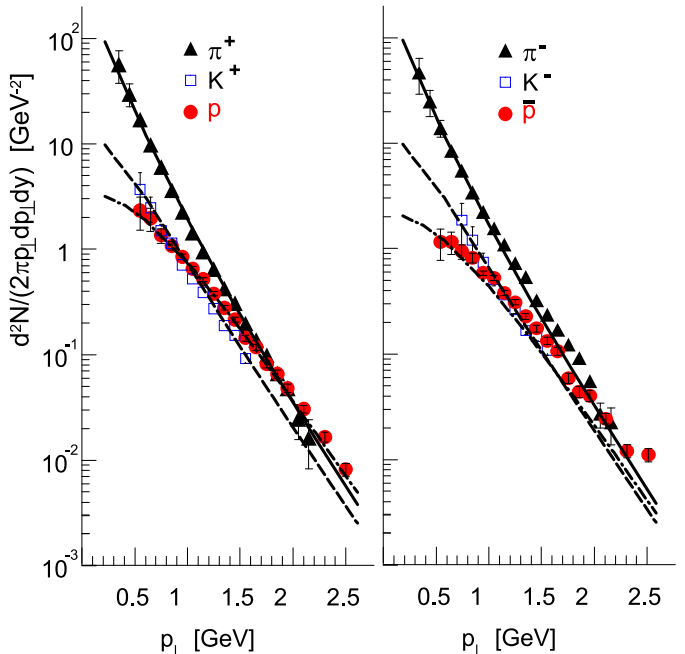


FIG. 1. The  $p_\perp$ -spectra of pions (solid line), kaons (dashed line) and protons or antiprotons (dashed-dotted line), as evaluated from our model with  $\rho_{\max}/\tau = 0.76$ , compared to the PHENIX preliminary data obtained from Fig. 1 of Ref. [1].

We now turn to a more detailed discussion of our approach. According to Eq. (1), the four-velocity of the hadronic fluid on the freeze-out surface is

$$u^\mu = \partial^\mu \tau = \frac{x^\mu}{\tau} = \frac{t}{\tau} \left( 1, \frac{r_z}{t}, \frac{r_x}{t}, \frac{r_y}{t} \right). \quad (2)$$

We use the following parametrization [14]:

$$\begin{aligned} t &= \tau \cosh \alpha_{\parallel} \cosh \alpha_{\perp}, & r_z &= \tau \sinh \alpha_{\parallel} \cosh \alpha_{\perp}, \\ r_x &= \tau \sinh \alpha_{\perp} \cos \phi, & r_y &= \tau \sinh \alpha_{\perp} \sin \phi, \end{aligned} \quad (3)$$

where  $\alpha_{\parallel}$  is the rapidity of the fluid element ( $v_z = z/t = \tanh \alpha_{\parallel}$ ), whereas  $\alpha_{\perp}$  describes the transverse size of the system ( $\rho = \tau \sinh \alpha_{\perp}$ ). The transverse velocity is  $v_{\rho} = \tanh \alpha_{\perp} / \cosh \alpha_{\parallel}$ , thus the model has *transverse flow*.

The particle densities are obtained as the integrals over the freeze-out hyper-surface [18]

$$N_i = \int \frac{d^3 p}{p^0} \int p^{\mu} d\Sigma_{\mu} f_i(p \cdot u), \quad (4)$$

where  $d\Sigma_{\mu}$  is the volume element of the hyper-surface (1),  $f_i$  is the phase-space distribution function for particle species  $i$ , and  $p^{\mu}$  is the four-momentum,

$$p^{\mu} = (m_{\perp} \cosh y, m_{\perp} \sinh y, p_{\perp} \cos \varphi, p_{\perp} \sin \varphi). \quad (5)$$

With help of parametrizations (3) and (5) we find the rapidity and transverse-momentum distributions of hadrons,

$$\frac{dN_i}{d^2 p_{\perp} dy} = \tau^3 \int_{-\infty}^{+\infty} d\alpha_{\parallel} \int_0^{\rho_{\max}/\tau} \sinh \alpha_{\perp} d(\sinh \alpha_{\perp}) \times \int_0^{2\pi} d\xi p \cdot u f_i(p \cdot u), \quad (6)$$

where

$$p \cdot u = m_{\perp} \cosh(y - \alpha_{\parallel}) \cosh \alpha_{\perp} - p_{\perp} \cos \xi \sinh \alpha_{\perp}, \quad (7)$$

and  $\xi = \phi - \varphi$ . We observe that the rapidity distribution (6) is boost-invariant, since the dependence on  $y$  can be absorbed in the integration variable by shifting  $\alpha_{\parallel} \rightarrow \alpha_{\parallel} + y$ . Clearly, this is a direct consequence of the assumed boost-invariant form of the freeze-out surface.\*

In the standard thermal-model fits of particle ratios one assumes that the fluid element is at rest, and the particles are collected from whole phase space. In other words, one computes the integrals  $N_i = V \int d^3 p f_i(\sqrt{m_i^2 + p^2})$ . The question arises whether the ratios obtained that way are the same as the ratios for multiplicities experimentally collected in the mid-rapidity region, *i.e.*, the ratios of the integrals  $dN_i/dy = \int d^2 p_{\perp} dN_i/(d^2 p_{\perp} dy)$ . The answer is yes, and follows from the boost-invariance of the expansion model. Indeed, since  $dN_i/dy$  are independent of  $y$ , we have

$$\frac{dN_i/dy}{dN_j/dy} = \frac{\int dy dN_i/dy}{\int dy dN_j/dy} = \frac{N_i}{N_j}. \quad (8)$$

This obvious general result can be verified explicitly in our specific boost-invariant model. The rapidity density

is given by the expression where the integral over  $\alpha_{\perp}$  factorizes:

$$\begin{aligned} \frac{dN_i}{dy} &= \tau^3 \int d^2 p_{\perp} \int_{-\infty}^{+\infty} d\alpha_{\parallel} \int_0^{\rho_{\max}/\tau} \sinh \alpha_{\perp} d(\sinh \alpha_{\perp}) \\ &\quad \times \int_0^{2\pi} d\xi p \cdot u f_i(p \cdot u) \\ &= 2\pi \tau^3 \int_0^{\rho_{\max}/\tau} \sinh \alpha_{\perp} d(\sinh \alpha_{\perp}) \\ &\quad \times \int \frac{d^3 p'}{E'} E'' f_i(E'') \\ &= \pi \rho_{\max}^2 \tau \int d^3 p'' f_i\left(\sqrt{p''^2 + m_i^2}\right), \end{aligned} \quad (9)$$

where we have performed two subsequent changes of variables:  $p'_z = \sqrt{p_x^2 + p_y^2 + m_i^2} \sinh \alpha_{\parallel}$ ,  $p'_x = p_x$ ,  $p'_y = p_y$ ,  $E' = \sqrt{p_x'^2 + p_y'^2 + p_z'^2 + m_i^2}$ , and  $E'' = E' \cosh \alpha_{\perp} - p'_x \sinh \alpha_{\perp}$ ,  $p''_x = p'_x \cosh \alpha_{\perp} - E' \sinh \alpha_{\perp}$ ,  $p''_y = p'_y$ ,  $p''_z = p'_z$ . Note that the passage to the double-primed variables is equivalent to the boost transformation to the local rest frame of the fluid element. Eq. (9) verifies explicitly the fact that  $dN_i/dy = \text{const} \times N_i$  (see also Ref. [19], where the Boltzmann distribution functions are discussed in a similar context). The results (8) or (9) are crucial, since they mean that in our analysis we can use the values of the temperature and chemical potentials as found in Ref. [11]. Moreover, to obtain the  $p_{\perp}$ -spectra from Eq. (6) we may use the form of the functions  $f_i(\varepsilon)$  which is exactly the same as obtained in [11]. We recall here that the shape of  $f_i(\varepsilon)$  is determined by the thermal component and by additional contributions from all decaying heavier resonances. Since  $f_i(\varepsilon)$  is a scalar function, we calculate it in the local rest frame of the fluid element and subsequently make the substitution  $\varepsilon \rightarrow p \cdot u$ .

We note that the time scale at which the resonances decay is, for most cases, of the order of  $1/\Gamma \sim 1 - 2$  fm, sufficiently less than the typical time scale of the hydrodynamic expansion,  $\tau \sim$  a few fm. This validates the approximation where the resonances decay at the freeze-out hyper-surface. The parameter  $\tau$  is determined within our approach by fitting the normalization of curves in Fig. 1. This yields  $\tau \simeq 6$  fm. On the other hand, the PHOBOS [20] multiplicity measurements at mid-rapidity and highest centrality, together with Eq. (6), imply  $\tau \simeq 9$  fm. The discrepancy may be due to the difference in the centrality of collisions, or problems in the normalization of preliminary experimental data. We compare to the minimum-bias data of PHENIX, since presently these are available for more types of particles. These data average over centralities, and thus our analysis may be viewed as an average over the impact parameter. We wish to point out that the normalization is not essential for our study of the shape and relative strengths of the  $p_{\perp}$ -spectra. The quantity  $\tau^3$  enters only as an overall

\*Since deviations from the boost-invariance are seen in the rapidity distributions [3], our present approach should be regarded as an approximate description of the mid-rapidity region.

scale in Eq. 6.

In Fig. 1 we show our main result. The  $p_\perp$ -spectra of pions, kaons, protons and antiprotons, evaluated from Eq. (6) with  $\tau = 6$  fm and  $\rho_{\max}/\tau = 0.76$ , are compared to the recent PHENIX data [1]. We observe a very good agreement of our model with the data up to  $p_\perp \sim 2$  GeV for  $\pi^\pm$ ,  $K^\pm$ , and  $p$ , and up to  $p_\perp \sim 1$  GeV for  $\bar{p}$ . In that range the model curves cross virtually all data points within the error bars. At larger values of  $p_\perp$ , where hard processes are expected to contribute, the model falls below the data for  $p$  and  $\bar{p}$ . Since the values of the strange and isospin chemical potentials are very close to zero, the model predictions for  $\pi^+$  and  $\pi^-$ , as well as for  $K^+$  and  $K^-$  are virtually the same. The value of the baryon chemical potential of 41 MeV splits the  $p$  and  $\bar{p}$  spectra. Note the convex shape of the pion spectra. The  $\pi^+$  and  $p$  curves in Fig. 1 cross at  $p_\perp \simeq 2$  GeV, and the  $K^+$  and  $p$  at  $p_\perp \simeq 1$  GeV, exactly as in the experiment.

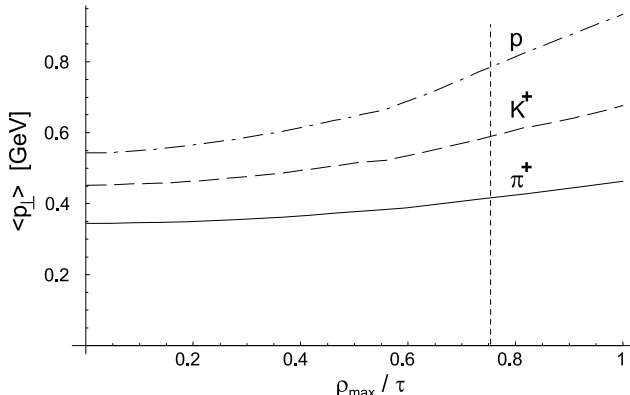


FIG. 2. The mean transverse momenta,  $\langle p_\perp \rangle$ , plotted as a function of the transverse size  $\rho_{\max}/\tau$ . The dashed vertical line indicates the best-fit value  $\rho_{\max}/\tau = 0.76$ .

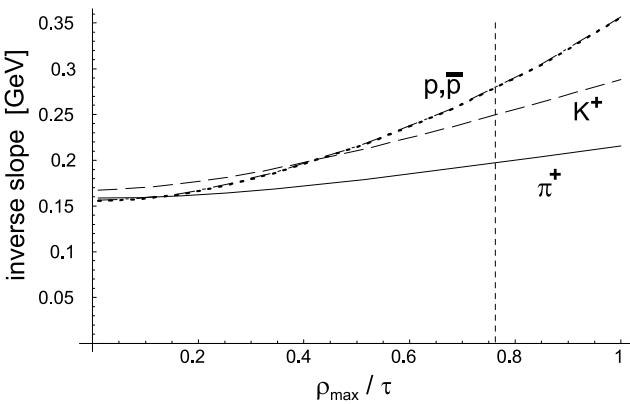


FIG. 3. The slope parameters,  $T_{\text{eff}}$ , defined in the text, plotted as a function of the transverse size  $\rho_{\max}$ . The dashed vertical line as in Fig. 2.

In Fig. 2 the values of  $\langle p_\perp \rangle$  are shown as a function of  $\rho_{\max}$ . For larger values of  $\rho_{\max}$  the transverse flow is stronger and the mean transverse momenta in-

crease. Also, the increase of mass of the particle leads to a larger  $\langle p_\perp \rangle$ . The numerical values at  $\rho_{\max}/\tau = 0.76$  agree within error bars with the values given on Fig. 4 of Ref. [1].

A popular measure of the spectra is the inverse-slope parameter obtained from fitting the spectra to the exponential form  $\exp(-m_\perp/T_{\text{eff}})$ . This measure, complementary to  $\langle p_\perp \rangle$ , is somewhat biased, since it depends on the choice of the fitting region in  $p_\perp$ . Following Ref. [1], we choose  $0.3\text{GeV} < p_\perp < 0.9\text{GeV}$  for the pions, and  $0.55\text{GeV} < p_\perp < 1.6\text{GeV}$  for the other particles. The results are shown in Fig. 3. The values at the best-fit value of  $\rho_{\max}/\tau = 0.76$  agree with the values of Ref. [1] within error bars.

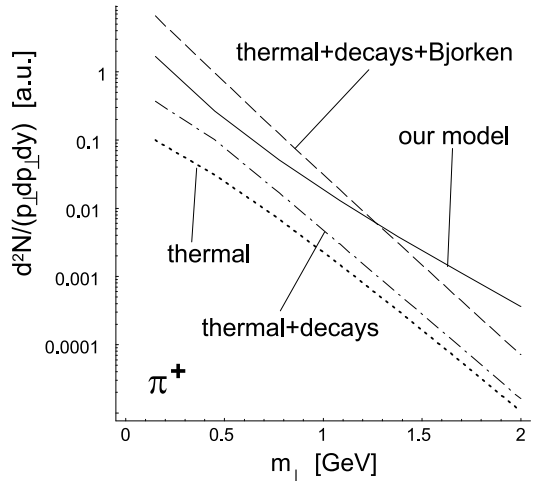


FIG. 4. Contributions of various effects to the  $p_\perp$ -spectra of  $\pi^+$  (normalizations arbitrary).

We end this paper with a more pedagogical discussion of the role of various effects included in our analysis. In Fig. 4 the dotted line shows the pion  $p_\perp$ -spectrum in a static fireball with the same temperature and chemical potentials as used in our calculation. No secondary decays are included in this case. The effect of the secondary decays of *all* resonances is represented by the dashed-dotted line. Decays of the resonances lead to an effective decrease of the temperature by about 35-40 MeV [11], since the emitted particles tend to populate the low- $p_\perp$  region. However, the spectrum remains concave. The effect of the pure longitudinal Bjorken expansion (with  $\tau = \sqrt{t^2 - r_z^2} = \text{const}$ ) is illustrated by the dashed line. This is a *redshift* effect, since all fluid elements move away from the observer, which leads to extra cooling of the spectrum. The solid line corresponds to our model, incorporating both the longitudinal expansion and the transverse flow. The transverse flow causes some fluid element to move in the direction of the observer, leading to *blueshift* [21]. Hence we find a combination of redshift and blueshift, yielding the  $p_\perp$  spectrum displayed by the solid line if Fig. 3. Note that the spectrum finally ac-

quires the convex shape, as seen in the experiment (*cf.* Fig. 1). The effects of blueshift are stronger for more massive particles, hence the behavior of Figs. 1, 2, and 3.

To conclude, we emphasize that the presented model, implementing in a simple fashion all key ingredients: freeze-out, decays of resonances, and longitudinal and transverse flows, works for RHIC. We stress that we do not need to introduce separate chemical and thermal freeze-outs. In other words, it is not necessary to have particle rescattering after the freeze-out, or to incorporate adiabatic cooling, *etc.* Our results give hints for more complicated hydrodynamic calculations, by providing the freeze-out conditions that describe the data. The natural extensions of the model should include different centrality effects (elliptic flow), and rapidity dependence. We have checked that the model works also for the SPS data. The details of this study will be presented elsewhere.

---

- [19] J. Cleymans, H. Oeschler, and K. Redlich, *J. Phys. G* **25**, 281 (1999).
- [20] B. B. Back *et al.*, PHOBOS Collaboration, *Phys. Rev. Lett.* **85**, 3100 (2000).
- [21] U. Heinz, *Nucl. Phys. A* **661**, 140 (1999).

- [1] J. Velkovska for the PHENIX Collaboration, *nucl-ex/0105012*.
- [2] A. Bazilevsky for the PHENIX Collaboration, *nucl-ex/0105017*.
- [3] Proceedings of the *Quark Matter 2001* conference, Brookhaven National Laboratory, January 2001, *Nucl. Phys. A* (in print).
- [4] P. Braun-Munzinger, J. Stachel, J. P. Wessels, and N. Xu, *Phys. Lett. B* **344**, 43 (1995); *Phys. Lett. B* **365**, 1 (1996).
- [5] J. Rafelski, J. Letessier, and A. Tounsi, *Acta Phys. Pol. B* **28**, 2841 (1997).
- [6] J. Cleymans, D. Elliott, H. Satz, and R. L. Thews, *Z. Phys. C* **74**, 319 (1997)
- [7] P. Braun-Munzinger, I. Heppe, and J. Stachel, *Phys. Lett. B* **465**, 15 (1999).
- [8] G. D. Yen and M. I. Gorenstein, *Phys. Rev. C* **59**, 2788 (1999).
- [9] M. Ga  dzicki, *Nucl. Phys. A* **681**, 153 (2001).
- [10] P. Braun-Munzinger, D. Magestro, K. Redlich, and J. Stachel, *hep-ph/0105229*.
- [11] W. Florkowski, W. Broniowski, and M. Michalec, *nucl-th/0106009*.
- [12] J. Dolej  , W. Florkowski, and J. H  fner, *Phys. Lett. B* **349**, 18 (1995).
- [13] J. D. Bjorken, *Phys. Rev. D* **27**, 140 (1983).
- [14] T. Cs  rg   and B. L  rstad, *Phys. Rev. C* **54**, 1390 (1996).
- [15] R. Scheibl and U. Heinz, *Phys. Rev. C* **59**, 1585 (1999).
- [16] J. Sollfrank, P. Koch, and U. Heinz, *Phys. Lett. B* **252**, 256 (1990).
- [17] G. E. Brown, J. Stachel, and G. M. Welke, *Phys. Lett. B* **253**, 19 (1991).
- [18] F. Cooper, G. Frye, and E. Schonberg, *Phys. Rev. D* **11**, 192 (1975).